PERGAMON

Available online at www.sciencedirect.com

SCIENCE DIRECT®

Polyhedron 22 (2003) 2457–2461

POLYHEDRON

www.elsevier.com/locate/poly

Magnetic properties of maghemite nanoparticles in a polyvinylpyridine matrix

Ian Gilbert [a,*], Angel Millán [a], Fernando Palacio [a], Andrea Falqui [b], Etienne Snoeck [b], Virginie Serin [b]

[a] *Instituto de Ciencia de Materiales de Aragón, CSIC-Universidad de Zaragoza, 50009 Zaragoza, Spain*
[b] *CEMES-CNRS, Toulouse, France*

Received 1 November 2002; accepted 28 December 2002

Abstract

Magnetic measurements have been carried out on nanocomposites consisting of individual maghemite (γ-Fe_2O_3) particles distributed throughout a polyvinylpyridine matrix with a range of particle sizes and concentrations. Magnetic measurements and particle size measurements have been compared to investigate particle size effects upon magnetic properties. Magnetisation increases slowly with increasing iron content up to approximately 18%, at which point the increase becomes sharper. Magnetic moment, as derived from a modified Langevin equation, is found to be less than the value expected from the particle, indicating possible surface effects. Blocking temperatures have been observed to increase with increasing iron concentration. Assuming no significant particle interactions it is possible to consider the effective anisotropy of individual particles. Effective anisotropy has been observed to increase with decreasing particle size, implying an increase in contribution from surface effects, and increases with the presence of rod shaped particles, implying a contribution from shape anisotropy.

Keywords: Nanocomposite; Polyvinylpyridine; Maghemite; Nanoparticles; Magnetic properties

1. Introduction

Recent years have seen a great interest in the production, characterisation and application of magnetic nanoparticles. Much of the early literature focussed on nanoparticles and their properties as constituents of ferrofluids [1–5], and more recently, where nanoparticles have been dispersed within a polymer matrix, the particles were produced separately [6,7]. Here we report the magnetic properties of maghemite nanoparticles produced directly within a polyvinylpyridine matrix. Characterisation of the magnetic properties is greatly influenced by the size and distribution of particles within their dispersion media. Indeed, the dispersion media itself has been observed to affect the magnetic properties [1,8–10]. As particle size decreases the surface/volume ratio of atoms increases giving increasing importance to surface events. Finite size effects and spin canting [4,6,10–12] have been investigated to explain the deviation of magnetic properties from the bulk behaviour as we decrease the particle size from tens of nanometers down to 2–4 nm. Deviation from the bulk has also been accounted for by considering the distribution of particle sizes produced, as well as anisotropic effects, again due to the increase in contribution from a surface anisotropy and also a shape anisotropy from non-spherical particles.

2. Experimental

Samples were produced using a novel preparation route with a range of iron contents (Table 1) [13]. The method is based on the hydrolysis of iron (III) salts in the presence of monovalent halide such that an iron halide complex ion should be formed in solution. The forced hydrolysis of these complex solutions yields a precipitate that, after washing and drying, consists of

* Corresponding author.
E-mail address: igilbert@posta.unizar.es (I. Gilbert).

0277-5387/03/$ - see front matter
doi:10.1016/S0277-5387(03)00246-8

Table 1
Summary of the properties of the samples produced in this study

	%Fe	Mean particle volume (nm^3)	μ_1 (μ_B)	μ_2 (μ_B)	Curie constant, C (emu K g^{-1})	Weiss constant θ (K)	Effective anisotropy K_{eff} ($\times 10^4$ Jm^{-3})
Rb0.1	5.33	33.0	192	441	0.49	44.98	2.699
Rb0.25	11.5	49.6	199	433	–	–	2.032
Rb0.3	13.0	–	139	278	0.04	162.5	–
Rb0.35	14.5	–	228	713	0.12	221.0	–
Rb0.4	16.0	–	250	1588	0.23	176.9	–
Rb0.45	17.5	–	393	2606	0.67	107.3	–
Rb0.5	19.4	162	3390	7196	–	–	5.115
Rb1	21.7	119	3359	6208	–	–	11.290

μ_1 is the moment calculated from the Langevin fit. μ_2 is the moment calculated from the modified Langevin fit. The Curie constant and Weiss constant are those taken at 10 Hz over the temperature range 320–360 K.

maghemite nanoparticles. This method has been used to produce maghemite/polyvinylpyridine nanocomposite samples. These samples were characterised by DC magnetometry (0–50 kOe) and AC susceptibility (0.1–852 Hz) measurements using a Quantum Design SQUID magnetometer. Transmission electron microscopy has been used to determine the particle size distribution.

3. Results and discussion

3.1. Particle size distribution

A micrograph of a low iron content sample is presented in Fig. 1 and shows a well dispersed population of spherical particles. A log-normal distribution of particles has been observed for two low iron content samples (Rb0.1 and Rb0.25), and two higher iron content iron samples (Rb0.5 and Rb1). The higher iron content samples have two particle shapes present, spherical and rod, while the lower iron content samples contain just spherical particles. The average particle volumes (Table 1) increase as the iron content is increased up to 19.4%. A decrease in volume is then observed, and explained by the fact that the rod shaped particles form preferentially at the expense of the spherical particles. As such, the spherical particles in Rb0.5 are larger than those in Rb1, and although there are larger rod shaped particles in Rb1, the average volume of the particles is smaller.

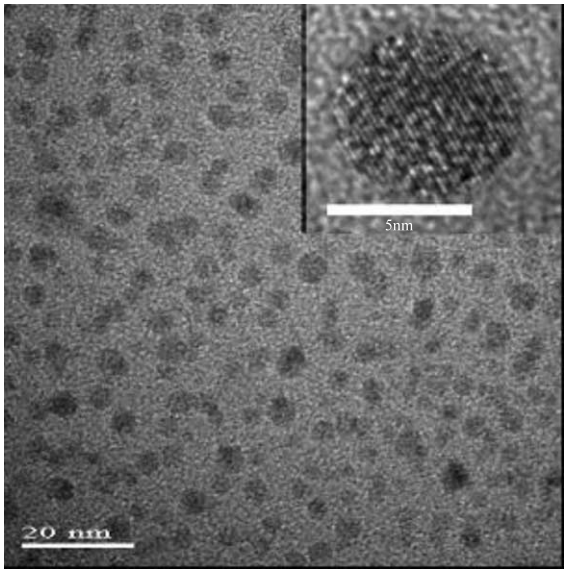

Fig. 1. Micrograph showing the distribution of spherical particles in a sample with an iron content of 5%.

3.2. DC magnetisation

DC magnetisation curves for the samples at 150 K are represented in Fig. 2. From superparamagnetic theory, the magnetisation of an isolated particle can be described by a Langevin equation:

$$M = M_0\left[\coth\left(\frac{\mu H}{kT}\right) - \frac{kT}{\mu H}\right]$$

where M_0 is the saturation magnetisation and μ the average magnetic moment. As such, we have attempted to fit our magnetisation data to this function (Fig. 2). Close agreement between the Langevin equation and the data was observed at low concentrations of iron, but deviated from this as concentration increased. This deviation can be accredited to many factors including, a particle size distribution [1,2,7], anisotropy effects [3], and surface effects [6,10,11]. A modified Langevin equation [14–16], which includes a linear contribution from the applied field to magnetisation, has also been used to fit our data (Fig. 3),

$$M = M_0\left[\coth\left(\frac{\mu H}{kT}\right) - \frac{kT}{\mu H}\right] + \chi H$$

This equation was originally applied to ferritin nanoparticles [14], and it was suggested that the extra linear term is related to superantiferromagnetic behaviour. However, the improved fit to our data indicates

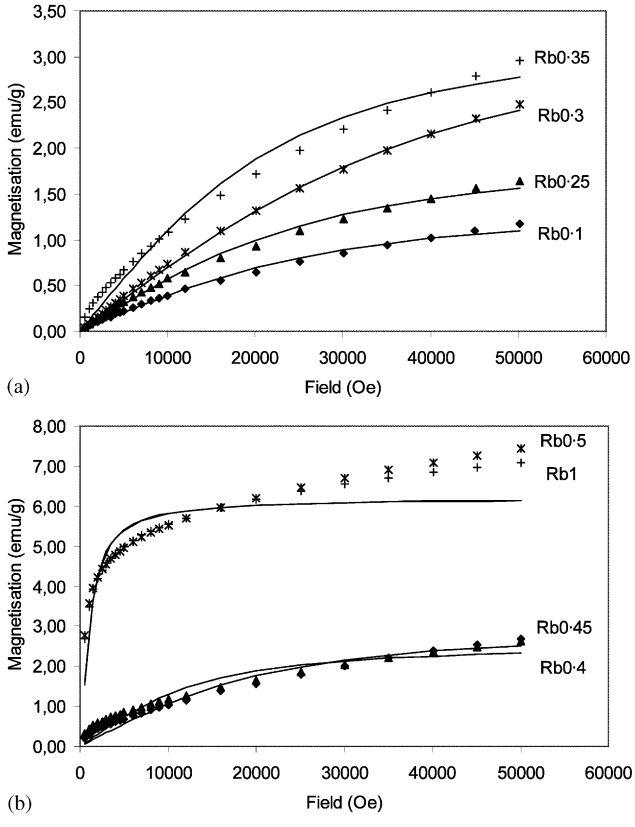

Fig. 2. Magnetisation data at 150 K for samples with a curve representing a Langevin fit for (a) low iron content, and (b) higher iron content.

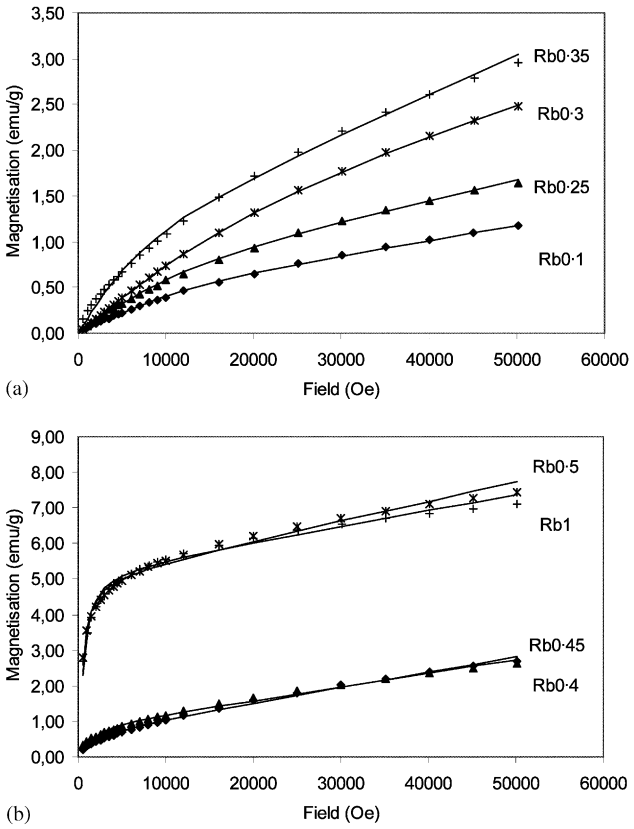

Fig. 3. Magnetisation data at 150 K for samples with a curve representing a modified Langevin fit for (a) low iron content, and (b) higher iron content.

that this extra term can also account for the paramagnetic contribution from the matrix.

Magnetic moment was calculated for the samples and found to be much lower than the value expected for the low iron content samples with small particle size. As particle size decreases, the surface/volume ratio increases such that surface events strongly affect the magnetic properties. Effects of spin canting or even a non-contributory surface layer will greatly reduce the moment of the particle and the observed magnetisation [3,4,10,12].

3.3. Curie–Weiss analysis

From the in-phase susceptibility (χ') measurements carried out with an applied field of 1 Oe, a standard Curie–Weiss analysis was conducted (Fig. 4) by extrapolating from the high temperature data, well above the blocking temperature. The parameters C and θ, where C is the Curie constant and θ is the Weiss constant, are presented in Table 1. Conclusions drawn from this analysis should be made with care. Closer examination of the 'linear' regions in relation to a wider temperature range in many cases has revealed a slight curvature [17–19], and in some cases, 'linear' regions were only observed after corrections made for thermal variations [5,8]. Samples presented here exhibit 'linear' regions, albeit over different temperature ranges. For comparison the data presented in Table 1 has been determined after extrapolation over the same temperature range in each sample.

As temperature is increased samples Rb0.3–Rb0.45 (Fig. 4(b)) exhibit a change in the gradient of the curve, similar to that previously observed in the literature where it has been interpreted as two distinct linear regions, one starting just above the blocking temperature, and the other occurring at much higher temperatures. This change has been attributed to both the temperature dependence of saturation magnetisation [6,8,20,21], and particle size distribution and interactions [5,16,22]. The particles produced in the samples for this study are well dispersed in the polymer matrix and is felt that the effects of interactions are negligible. Data for the Rb0.1 and Rb0.25 (Fig. 4(a)) exhibit different behaviour in that between the two linear regions, there is a third linear region of lesser gradient. The source of this behaviour is unclear and could have been explained by a double peak in the particle size distribution. However, we have already determined that a double peak does not exist for these two samples. We are currently working toward a clear interpretation of this behaviour.

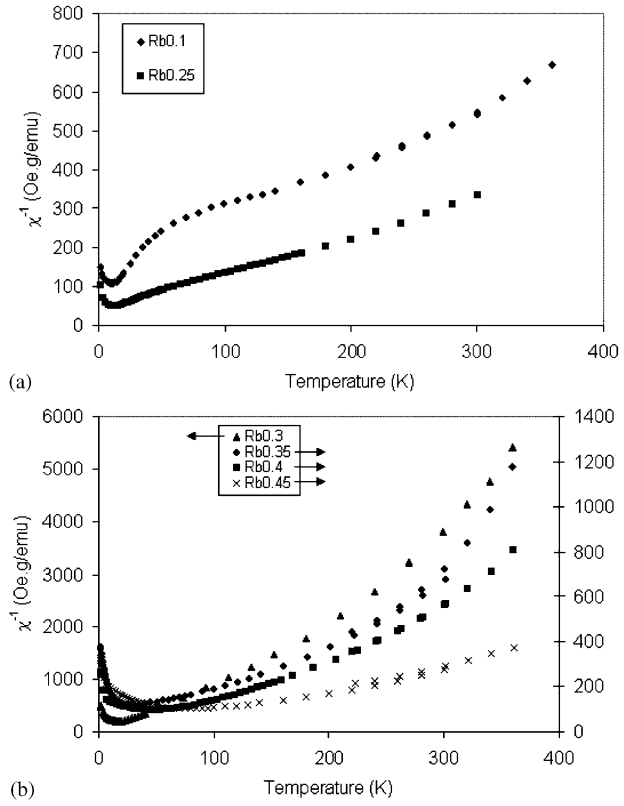

Fig. 4. Inverse AC susceptibility with an applied field of 1 Oe for samples (a) Rb0.1 and Rb0.25, and (b) Rb0.3–Rb0.45.

3.4. AC susceptibility

The out of phase susceptibility curves exhibit an increase in blocking temperature with increasing iron content, as can be observed from the normalised χ'' data in Fig. 5. For non-interacting particles, the time required for the reversal of the direction of magnetisation is described by the Néel–Arrhenius relation [23]:

$$\tau = \tau_0 e^{\left(\frac{E}{k_b T}\right)}$$

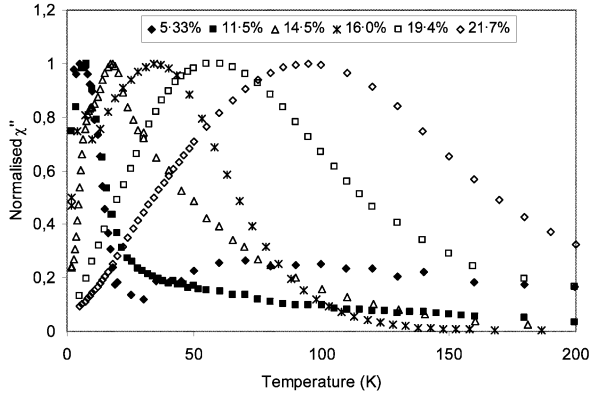

Fig. 5. Normalised out of phase susceptibility exhibiting increase in blocking temperature with increasing iron content.

where τ_0 is a time constant related to the measuring frequency, E is the anisotropy energy barrier, k_b is the Boltzmann constant and T is the absolute temperature. Taking the energy barrier as a maximum at the blocking temperature, T_b, and using a plot of $\ln(\tau)$ as a function of reciprocal blocking temperature, an average value of 4.365×10^{-12} s for τ_0 was determined over all the samples. This falls within the wide range of values previously reported in the literature (10^{-13}–10^{-9}) [9,10,14,24,25]. Much of the literature uses Mössbauer and magnetisation measurements to provide two different measurement frequencies in order to determine τ_0 [9,10]. Mössbauer typically having a measurement time in the order of 10^{-9} s, whereas for magnetisation measurements this is typically 100 s. Using AC susceptibility permits measurement over a range of frequencies, therefore providing more than just the two measurement times [14,24,25].

3.5. Energy barrier

It is generally accepted that the energy barrier to reversal of magnetisation is anisotropy related ($E = KV$, where K is the anisotropy constant and V is the particle volume). Within any 'real' system there is usually a distribution of particle sizes, each contributing to the overall energy by virtue of their individual volumes and anisotropies. Here we consider the energy to be a product of an effective anisotropy constant and an average particle volume. From the Néel–Arrhenius relation, we can determine a value for this effective energy barrier (Fig. 6). Overall it was observed that there is an increase in the effective energy with increasing iron content, this increase being gradual up to an iron content of 13%, and then suddenly becoming more pronounced. It is thought that up to 13% iron we have only a population of spherical particles and those samples with more iron start to form a population of rod shaped particles. The rod shaped particles, by virtue

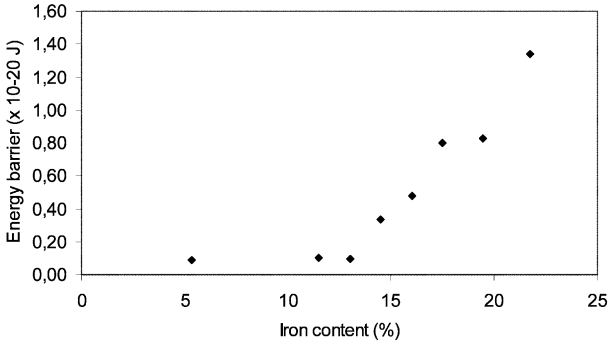

Fig. 6. Energy barrier calculated from Néel–Arrhenius relation at blocking temperature with increasing iron content.

of their shape anisotropy, will increase the energy barrier [11].

3.6. Effective anisotropy

The determination of the variation of the anisotropy is complex, and so for comparison, we represent here the effective anisotropy for the particles. Looking at our results (Table 1), we can see that for samples Rb0.1 and Rb0.25, where there are only spherical particles present, we observe this decrease in effective anisotropy, K_{eff} with increasing particle size. As particle size decreases, the ratio of surface to volume atoms increases. As such, we would expect a greater contribution from surface anisotropy with decreasing particles size, which is consistent with our samples and that previously reported in the literature [5,10,26,27]. For samples Rb0.5 and Rb.1 we observe larger values for K_{eff}, and that K_{eff} increases with the increase in iron content. Although the spherical particles in these samples are larger than those in the previous samples, and therefore should exhibit lower values of K_{eff}, there is also the presence of needle-shaped particles to consider. As such, it appears that the contribution from shape anisotropy is much greater than that from the surface/volume anisotropy.

4. Conclusions

A novel method for the direct production of maghemite nanoparticles within a polymer matrix has been used to produce samples with a range of particles sizes and distributions. For complete magnetic characterisation a combination of magnetic measurements and knowledge of the particle size, shape and distribution is required, as the latter is observed to strongly affect magnetic properties. As particle size decreases so does the surface/volume ratio, as such, surface effects dominate the magnetic properties. As the iron content increases, the volume of spherical particles increases. However the formation of rod-shaped particles soon becomes preferential at the expense of the spherical particles, as such, affecting the magnetic properties by virtue of a shape anisotropy.

References

[1] R. Kaiser, G. Miskolczy, J. Appl. Phys. 41 (1970) 1064.
[2] R.W. Chantrell, J. Popplewell, S.W. Charles, IEEE Trans. Mag. MAG-14 (1978) 975.
[3] M. Hanson, C. Johansson, S. Mørup, J. Phys.:Condens. Matter 5 (1993) 725.
[4] F.T. Parker, M.W. Foster, D.T. Margulies, A.E. Berkowitz, Phys. Rev B 47 (1993) 7885.
[5] M. Hanson, C. Johansson, M.S. Pedersen, S. Mørup, J. Phys.:-Condens. Matter 7 (1995) 9269.
[6] R. Cherkaoui, M. Noguès, J.L. Dormann, P. Prené, E. Tronc, J.P. Jolivet, D. Fiorani, A.M. Testa, IEEE Trans. Mag. 30 (1994) 1098.
[7] O. Jarjayes, P.H. Fries, G. Bidan, J. Mag. Mag. Mat. 137 (1994) 205.
[8] P. Prené, E. Tronc, J.P. Jolivet, J. Livage, R. Cherkaoui, M. Noguès, J.L. Dormann, IEEE Trans. Mag. 29 (1993) 2658.
[9] S. Mørup, C.A. Oxborrow, P.V. Hendriksen, M.S. Pedersn, M. Hanson, C. Johansson, J. Mag. Mag. Mat. 140–144 (1995) 409.
[10] E. Tronc, A. Ezzir, R. Cherkaoui, C. Chanéac, M. Noguès, H. Kachkachi, D. Fiorani, A.M. Testa, J.M. Grenèche, J.P. Jolivet, J. Mag. Mag. Mat. 221 (2000) 63.
[11] H. Kachkachi, A. Ezzir, M. Noguès, E. Tronc, Eur. Phys. J. B 14 (2000) 681.
[12] O. Iglesias, A. Labarta, Phys. Rev. B 63 (2001) 184416.
[13] A. Millán, F. Palacio, A. Falqui, E. Snoeck, V. Serin, Mater. Res. Soc. Symp. Proc. 733E (2002) T.5.2.1.
[14] S.H. Kilcoyne, R. Cywinski, J. Mag. Mag. Mat. 140–144 (1995) 1466.
[15] S.A. Makhlouf, F.T. Parker, A.E. Berkowitz, Phys. Rev. B: Rapid Comms. 55 (1997) R14717.
[16] M.S. Seehra, V.S. Babu, A. Manivannan, J.W. Lynn, Phys. Rev. B 61 (2000) 3513.
[17] M. Holmes, K. O'Grady, J. Popplewell, J. Mag. Mag. Mat. 85 (1990) 47.
[18] M. El-Hilo, K. O'Grady, R.W. Chantrell, J. Mag. Mag. Mat. 117 (1992) 21.
[19] K. O'Grady, M. El-Hilo, R.W. Chantrell, IEEE Trans. Mag. 29 (1993) 2608.
[20] J.I. Gittleman, B. Abeles, S. Bozowski, Phys. Rev. B 9 (1974) 3891.
[21] A. Ezzir, J.L. Dormann, H. Kachkachi, M. Noguès, M. Godhino, E. Tronc, J.P. Jolivet, J. Mag. Mag. Mat. 196–197 (1999) 37.
[22] M.S. Seehra, A. Punnoose, Phys. Rev. B 64 (2000) 132410.
[23] L. Néel, Ann. Geophys. 5 (1949) 99.
[24] T. Jonsson, J. Mattson, P. Norblad, P. Svedlindh, J. Mag. Mag. Mat. 168 (1997) 269.
[25] C. Cannas, G. Concas, D. Gatteschi, A. Falqui, A. Musinu, G. Piccaluga, C. Sangregorio, G. Spano, Phys. Chem. Chem. Phys. 3 (2001) 832.
[26] F. Bødker, S. Mørup, S. Linderoth, Phys. Rev. Lett. 72 (1994) 282.
[27] F. Gazeau, J.C. Bacri, F. Gendron, R. Perzynski, Y.u.L. Raikher, V.I. Stepanov, E. Dubois, J. Mag. Mag. Mat. 186 (1998) 175.